TEMPO as a Hydrogen Atom Transfer Catalyst for Transition Metal-Free Aerobic Dehydrogenation of Activated Alkanes to Alkenes

Tasuku Ito, Falk William Seidel, Xiongjie Jin,* Kyoko Nozaki*

ABSTRACT: 2,2,6,6-Tetramethylpiperidine-*N*-oxyl (TEMPO) has been extensively utilized as a radical scavenger or an oxidation catalyst. In contrast, TEMPO as a hydrogen atom transfer (HAT) catalyst has rarely been studied. Here, we report that TEMPO, as the HAT catalyst, homolytically cleaves benzylic or allylic C–H bonds to give the corresponding alkyl radicals. Benefited from the dual roles played by TEMPO as the HAT catalyst and the radical scavenger, the highly challenging aerobic dehydrogenation of activated alkanes to alkenes is successfully developed.

INTRODUCTION

Since its first synthesis by Lebelev and Kazarnovskii in 1960,[1] 2,2,6,6-tetramethylpiperidine-*N*-oxyl (TEMPO), a stable *N*-oxyl radical, has been recognized as a radical scavenger (Scheme 1a).[2] The existence of a radical intermediate is often suggested when addition of TEMPO retards a reaction.[2] Alternatively, TEMPO is widely used as an oxidation catalyst for the dehydrogenation of alcohols or amines.[3] One-electron oxidation of TEMPO affords 2,2,6,6-tetramethyl-1-oxo-piperidinium cation (TEMPO$^+$) intermediate, which serves as a hydride-transfer catalyst (Scheme 1b).[3] In contrast, the use of TEMPO as a hydrogen atom transfer (HAT) catalyst has rarely been studied in organic transformations.[4] Namely, abstraction of a neutral hydrogen atom from alkanes to generate alkyl radicals and 1-hydroxy-2,2,6,6-tetramethylpiperidine (TEMPOH) is rather difficult even for activated alkanes such as ethylbenzene. It is attributed to the relatively lower O–H bond dissociation energy of TEMPOH (70 kcal mol^{-1} in MeCN) compared to other well-studied HAT catalyst such as *N*-hydroxyphthalimide (NHPI) (89 kcal mol^{-1} in MeCN).[5]

Alkenes are versatile building blocks in synthetic chemistry, and their synthesis by dehydrogenation of alkanes is of great importance.[6] Molecular oxygen is an attractive oxidant because it produces H_2O as the sole co-product. However, aerobic dehydrogenation of alkanes is highly challenging because oxygenated products such as carbonyl compounds and/or alcohols are generated by autoxidation *via* alkyl radical intermediates, which results in the low selectivity to alkenes.[7] To the best of our knowledge, there is lack of a transition metal-free catalyst system for the dehydrogenation of alkanes to alkenes using molecular oxygen as the terminal oxidant in a selective manner.[8]

Herein, we demonstrate that TEMPO works as the HAT catalyst for the homolytic cleavage of benzylic or allylic

Scheme 1. Outline of this study

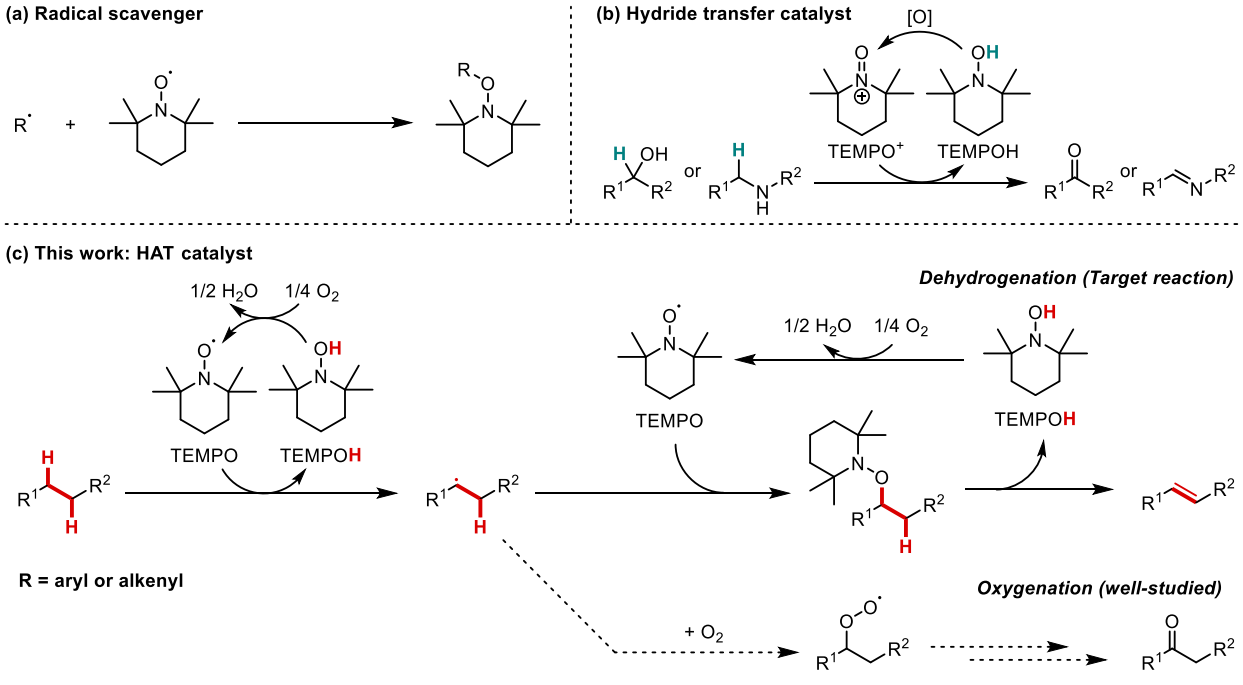

C−H bonds, leading to the formation of benzylic or allylic radicals from the corresponding alkyl arenes or cyclohexenes, respectively (Scheme 1c). The as-formed radical intermediates get rapidly trapped by TEMPO to form alkoxyamine intermediates. Elimination of TEMPOH from the alkoxyamine intermediate affords the corresponding alkenes. Notably, if the radical intermediate is trapped by molecular oxygen, undesired oxygenated products are given. The TEMPOH molecules generated during the process can be oxidized by molecular oxygen to regenerate TEMPO.[9] Thus, the dual role played by TEMPO, that is, as a HAT catalyst and a radical scavenger enabled the aerobic dehydrogenation of activated alkanes such as alkyl arenes or cyclohexenes to vinyl arenes or arenes, respectively.

RESULTS AND DISCUSSION

Optimization of the reaction conditions. When the dehydrogenation of ethylbenzene (**1a**) was carried out using 25 mol% of TEMPO as the catalyst at 100 °C under 1 atm of air for 72 h, only trace amounts of styrene (**2a**) and acetophenone (**3a**) were obtained (Table 1, entry 1). By raising the reaction temperature to 125 °C, the yield of **2a** was increased to 22% together with the formation of 9% yield of **3a**, and the ratio of **2a** to **3a** was 2.4/1 (Table 1, entry 2). 9-Azanoradamantane *N*-oxyl (nor-AZADO), a highly active catalyst for the oxidation of alcohols to carbonyl compounds,[10] resulted in the lower conversion of **1a** due to decomposition of the catalyst (Table 1, entry 3). When 5 mol% of NHPI, a well-known HAT catalyst for the generation of benzylic radicals from alkyl arenes,[11] together with 25 mol% of TEMPO was used as the catalyst, the yield of **2a** was not improved, which is likely due to the instability[12] of NHPI under the high reaction temperature (Table 1, entry 2 *vs* 4). Using 50 mol% of TEMPO resulted in the increase of the ratio to 8.8/1, and the yields of **2a**

Table 1. Aerobic dehydrogenation of ethylbenzene (1a) to styrene (2a) under various conditions[a]

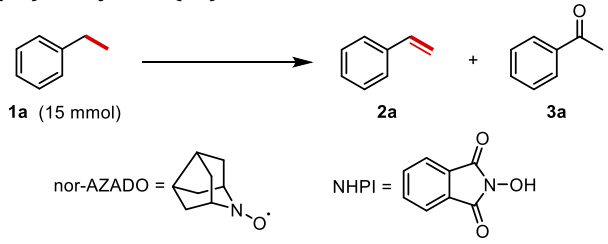

Entry	Catalyst (mol%)	Temp. (°C)	Conv. (%)[b]		Yield (%)[c]	
			1a	*N*-oxyl	**2a**	**3a**
1	TEMPO (25)	100	12	<1	1	2
2	TEMPO (25)	125	45	38	22	9
3	nor-AZADO (25)	125	19	>99	7	2
4	TEMPO (25) + NHPI (5)	125	41	40	14	12
5	TEMPO (50)	125	60	37	35	4
6	none	125	49	-	0	30

[a]Reaction conditions: **1a** (15 mmol, neat condition), air (1 atm), 72 h. [b]Conversion of **1a** was determined by NMR analysis using 1,3,5-trimethoxybenzene as an internal standard. Conversion of *N*-oxyl (TEMPO or nor-AZADO) was determined by GC analysis using 1,3,5-trimethoxybenzene as an internal standard, and calculated based on the added TEMPO. [c]**2a** and **3a** yields were determined by NMR analysis using 1,3,5-trimethoxybenzene as an internal standard.

Table 2. Substrate scope[a]

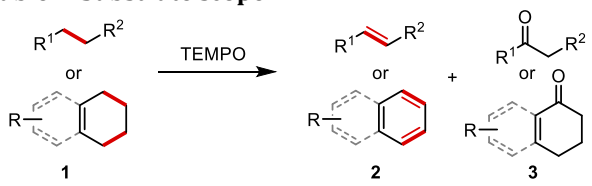

Entry	Substrate	*t* (h)	Conv. (%)	Yield of **2**/**3** (%)
1	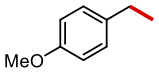	48	61	44/5
2	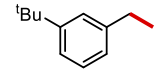	48	53	36/8
3	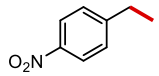	24	35	21/1
4	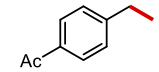	24	33	23/3
5	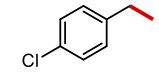	48	49	33/3
6	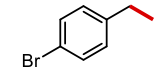	48	50	34/4
7	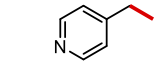	48	56	38/4
8	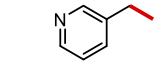	24	24	21/0
9	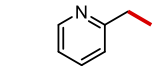	27	28	19/2
10	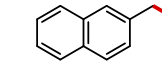	24	47	23/2
11[b]	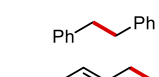	48	50	46/n.d.
12[b]	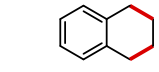	72	86	76/n.d.
13[b]	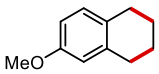	72	85	80/n.d.
14[b]	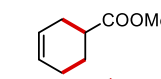	72	92	38/n.d.
15[b]	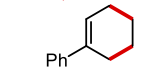	72	>99	47/n.d.
16[b,c]	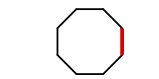	72	6	6/n.d.

[a]Reaction conditions: Substrate (15 mmol, neat condition), 130 ℃, air (1 atm). Yield and conversion were determined by NMR analysis using 1,3,5-trimethoxybenzene as an internal standard. n.d. = not detected. [b]yield and conversion were determined by GC analysis using 1,3,5-trimethoxybenzene as an internal standard. [c]145 ℃

and **3a** was 35% and 4%, respectively (Table 1, entry 5). This result can be explained by the enhancement of radical trapping rate with the increase of the TEMPO concentration which suppressed the reaction of molecule oxygen with the alkyl radicals (Scheme 1c). Since 2 equiv. of TEMPO is needed to dehydrogenate **1a** to **2a**, 35% yield of **2a** corresponds to the 3.8 equiv. to the consumed TEMPO. (Note: the conversion of TEMPO (37%) is calculated based on the added TEMPO, that is, 50 mol% with respect to **1a**). This result indicates that the present dehydrogenation does proceed catalytically, and molecular oxygen is the terminal oxidant. However, further elongation of reaction time did not improve the **2a** yield likely due to the side reactions such as oligomerization or polymerization of **2a** (Figure S1). When the reaction was carried out in the absence of TEMPO, only **3a** was obtained in 30% yield, which further supports the role of TEMPO to switch the pathway from autoxidation to dehydrogenation.

Substrate scope. Next, we examined the substrate scope of the reaction (Table 2, also see Scheme S2). First, the dehydrogenation of various substituted ethylbenzenes showed good functional group tolerance (Table 2, entries 1–6). The present dehydrogenation method was applicable to ethylbenzene substituted with either electron-donating or -withdrawing groups (Table 2, entries 1–6). Halogen-substituted ethylbenzenes were dehydrogenated leaving the halogen atoms untouched (Table 2, entries 5 and 6). The dehydrogenation also proceeded when using substrates having pyridine rings (Table 2, entries 7–9). In addition to the ethylbenzenes, 2-ethylnaphthalene was also dehydrogenated (Table 2, entry 10). An internal alkane, 1,2-diphenylethane was also dehydrogenated by applying the present dehydrogenation method (Table 2, entry 11). When using tetrahydronaphthalene either substituted or not as the substrate, double dehydrogenation proceeded to give the aromatized products in good yields (Table 2, entries 12 and 13). The dehydrogenation of substituted cyclohexenes also took place, and the corresponding arenes were obtained (Table 2, entries 14 and 15). The dehydrogenation of a simple alkane, cyclooctane, gave cyclooctene in 6% yield.

Table 3. Dehydrogenation of 4-ethylanisole (1b) under various conditions[a]

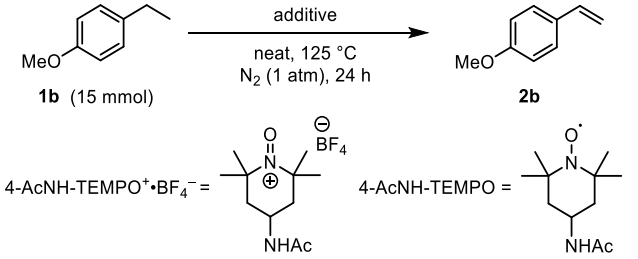

Entry	Catalyst (mol%)	Conv. of **1b** (%)	Yield of **2b** (%)
1	4-AcNH-TEMPO$^+$·BF_4^- (25)	< 1	n.d.
2	4-AcNH-TEMPO (25)	18	13

[a]Reaction conditions: **1b** (15 mmol, neat condition), N_2 (1 atm), 24 h. Conversion and yields were determined by NMR analysis using 1,3,5-trimethoxybenzene as an internal standard. n.d. = not detected.

Scheme 2. Radical clock experiment

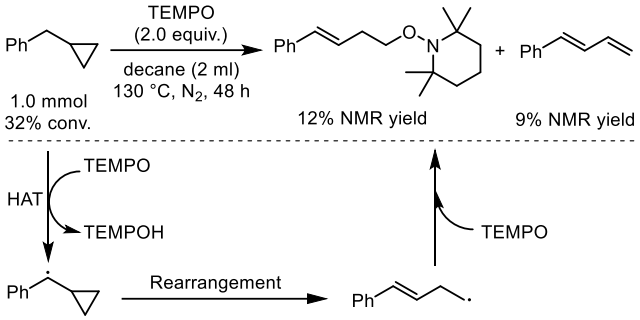

Mechanistic studies. First, we examined the possibility of the present dehydrogenation by an oxoammonium species as it has been reported to dehydrogenate cyclohexene to cyclohexa-1,3-diene *via* the hydride transfer process.[13] In our case, no conversion of 4-ethylanisole was observed when 4-acetamido-2,2,6,6-tetramethyl-1-oxopiperidinium tetrafluoroborate (4-AcNH-TEMPO$^+$·BF_4^-) was used for the dehydrogenation of 4-ethylanisole (**1b**) (Table 3, entry 1). On the other hand, 4-acetamide-2,2,6,6-tetramethylpiperidine-*N*-oxyl (4-AcNH-TEMPO), promoted the dehydrogenation of **1b** (Table 3, entry 2). The difference between 4-AcNH-TEMPO$^+$·BF_4^- and 4-AcNH-TEMPO in the dehydrogenation of **1b** supports the present dehydrogenation does not proceed through the conventional hydride transfer process by the oxoammonium species.

Different from the hydride transfer process, the present aerobic dehydrogenation proceeds through a radical intermediate formed by the TEMPO-catalyzed HAT process, as verified by the following experiments. When a radical clock, benzylcyclopropane, was reacted with 2 equiv. of TEMPO, ring opening of the cyclopropyl group occurred, and the corresponding alkoxyamine was obtained as the major product with the concomitant formation of the conjugated diene (Scheme 2). This result supports the formation of a benzylic radical intermediate *via* the TEMPO-

Scheme 3. Proposed reaction mechanism

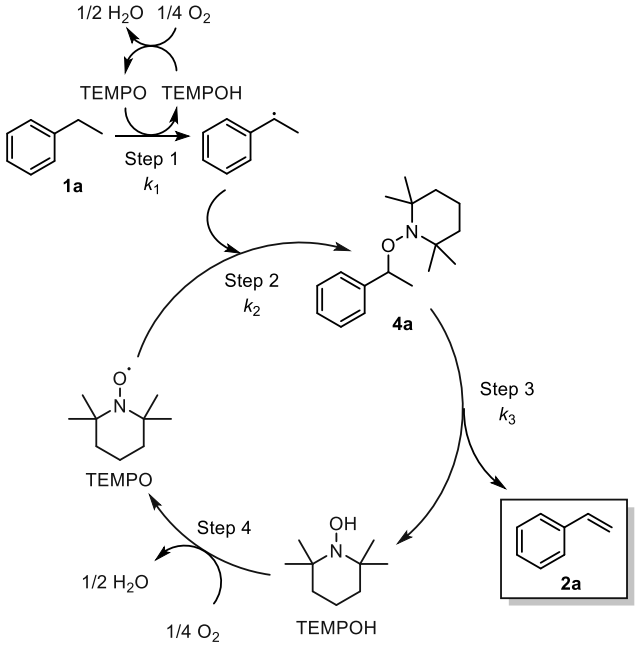

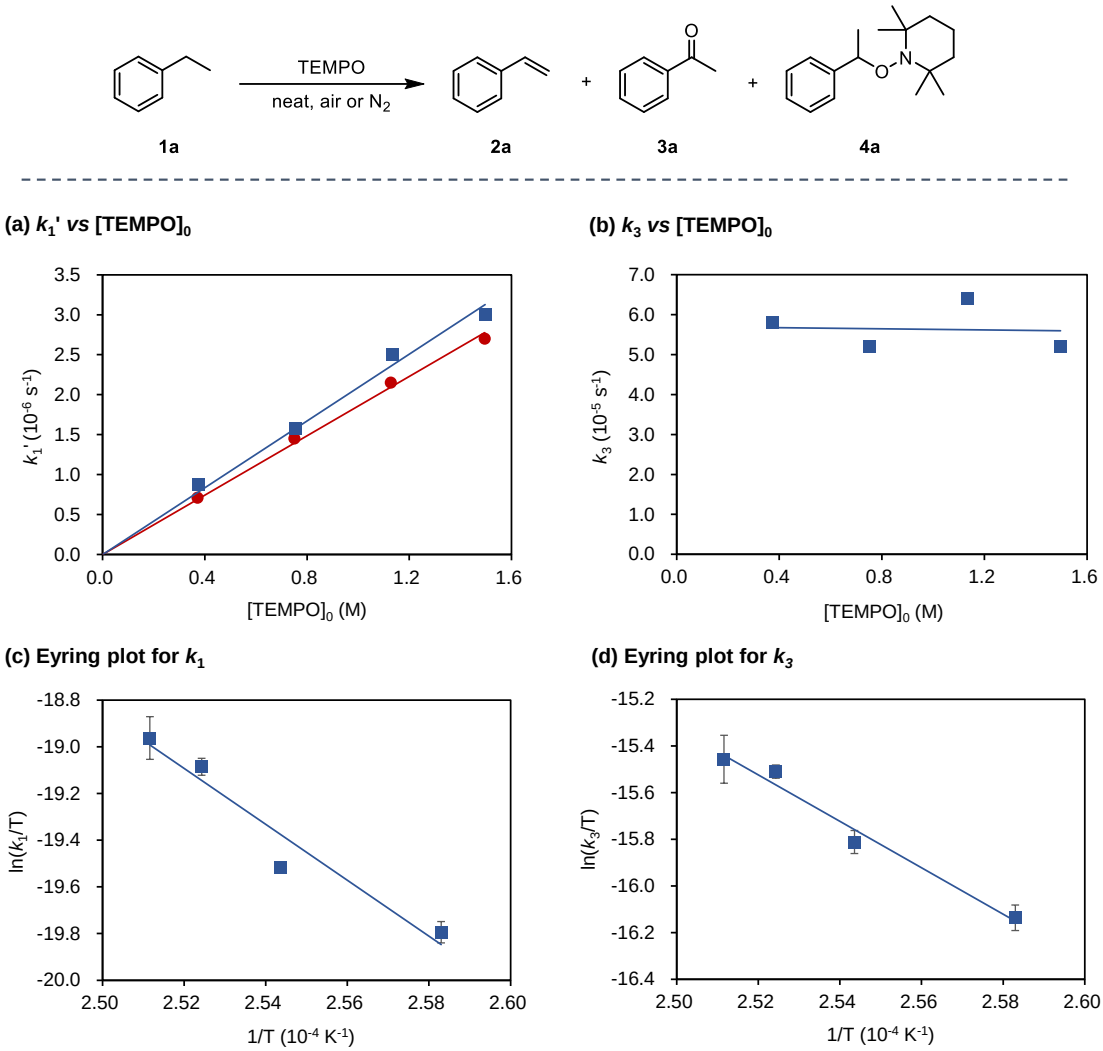

Figure 1. Kinetic studies. (a) Dependence of k_1' on $[\text{TEMPO}]_0$, line fit (N_2 atmosphere, blue line): $k_1' = 2.1 \times 10^{-6}[\text{TEMPO}]_0$ ($r^2 = 0.998$), line fit (under air, red line): $k_1' = 1.9 \times 10^{-6}[\text{TEMPO}]_0$ ($r^2 = 0.999$). (b) Dependence of k_3 on $[\text{TEMPO}]_0$ under N_2. (c) Eyring plot for k_1, line fit: $\ln(k_1/T) = -12.0 \times 10^4/T + 11.1$ ($r^2 = 0.939$). (d) Eyring plot for k_3, line fit: $\ln(k_3/T) = -10.0 \times 10^4/T + 9.6$ ($r^2 = 0.978$). Reaction conditions: (a), (b) **1a** (2.0 ml, 16.5 mmol), TEMPO (0.38–1.5 M), 125 ℃, N_2 or air (1 atm); (c), (d) **1a** (2.0 ml, 16.5 mmol), TEMPO (0.75 M), 114–125 ℃, N_2 (1 atm). Yields of **2a**, **3a**, and **4a** were determined by NMR analysis using 1,3,5-trimethoxybenzene as an internal standard.

catalyzed HAT process (Scheme 3, step1). When the dehydrogenation of **1a** was carried out under N_2, the corresponding alkoxyamine intermediate 2,2,6,6-tetramethyl-1-(1-phenylethoxy)piperidine (**4a**) was formed (Schemes 3 and S1), which also supports the dehydrogenation proceeds through an alkyl radical intermediate.

Based on the above results, a plausible reaction mechanism for the dehydrogenation of **1a** is illustrated in Scheme 3. First, TEMPO abstracts the hydrogen atom from the benzylic position of **1a** to form the benzylic radical intermediate (Scheme 3, step 1). Next, the generated benzylic radical is trapped by another TEMPO molecule to give the alkoxyamine intermediate **4a** (Scheme 3, step 2). Then, **4a** converts to the corresponding alkene and TEMPOH (Scheme 3, step 3).[14] Finally, TEMPOH is oxidized to regenerate TEMPO by molecular oxygen in air to complete the catalytic cycle (Scheme 3, step 4).[9]

We carried out kinetic studies for the dehydrogenation of **1a** to further verify the above proposed reaction pathway. The rate constants k_1–k_3 are defined for steps 1–3 in Scheme 3. By using these rate constants, the integrated rate equations for **1a**, **4a**, and **2a** at the initial stage of the reaction are shown as eqs. 1–3, where $k_1' = k_1[\text{TEMPO}]_0$ ($[\text{TEMPO}]_0$ is the initial concentration of TEMPO, for details on derivation of the integrated rate equations, see the supporting information). The rate constants k_1' and k_3 were obtained by fitting the initial stage of the reaction profiles with the integrated rate equations.

$$[\mathbf{1a}] = [\mathbf{1a}]_0 e^{-k_1' t} \quad \text{(eq. 1)}$$

$$[\mathbf{4a}] = [\mathbf{1a}]_0 \frac{k_1'}{k_3 - k_1'}\left(e^{-k_1' t} - e^{-k_3 t}\right) \quad \text{(eq. 2)}$$

$$[\mathbf{2a}] = [\mathbf{1a}]_0 \left\{1 + \frac{1}{k_1' - k_3}\left(k_3 e^{-k_1' t} - k_1' e^{-k_3 t}\right)\right\} \quad \text{(eq. 3)}$$

For the dehydrogenation of **1a** with various concentrations of TEMPO at 125 ℃ under N_2 or air atmosphere, k_1'

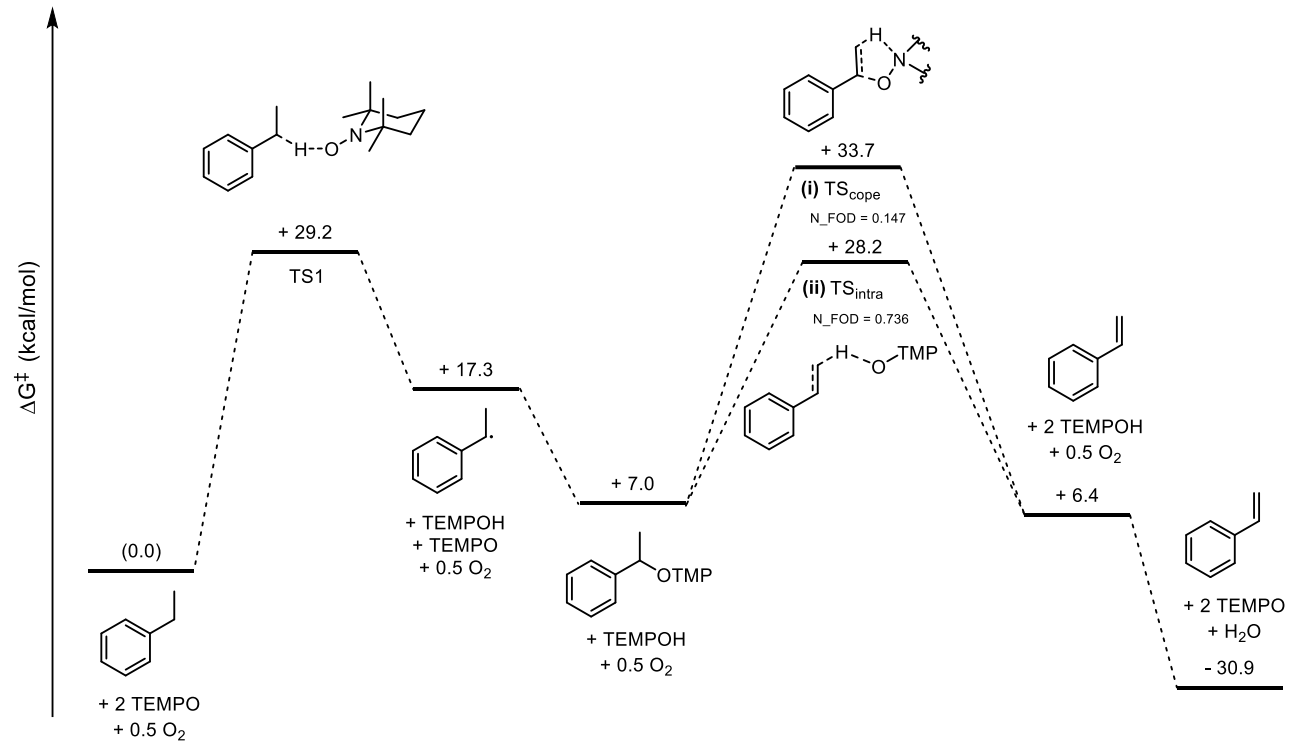

Figure 2. Computed free energy profiles for the aerobic dehydrogenation of **1a** to **2a**. The DFT Calculation was performed at FT-TPSS-D4 (5000K)/def2-TZVP//FT-PBE0-D4 (10000K)/def2-QZVPP) level of theory.

was lineally increased with the increase of $[TEMPO]_0$ (Figures 1a, S2a, and S2b). Thus, k_1 value was determined to be 2.1×10^{-6} M^{-1} s^{-1} (under N_2) or 1.9×10^{-6} M^{-1} s^{-1} (under air) (Figure 1a). The almost same value of k_1 either under N_2 or air indicates that TEMPO rather than molecular oxygen in air is responsible for the generation of the benzylic radical intermediate. On the other hand, the rate constant k_3 was almost constant under N_2 regardless of the change of TEMPO concentration (Figures 1b and S2a), which indicates that the conversion of the alkoxyamine intermediate to the corresponding alkene and TEMPOH proceeds through an intramolecular mechanism, and TEMPO was not involved in this step.

Then, kinetic analysis of the decomposition of the alkoxyamine intermediate **4a** was performed at 125 ℃ under N_2 (Figure S2c). By using **4a** as the substrate, the decomposition rate constant was determined to be 4.6×10^{-5} s^{-1} which is almost the same as the rate constant k_3 obtained from the aforementioned fitting results for the dehydrogenation of **1a** at 125 ℃ under N_2 ($k_3 = 5.7\pm0.5\times10^{-5}$ s^{-1}) (Figures 1b and S2a). Therefore, the identified alkoxyamine **4a** is indeed the reaction intermediate, and the decomposition of **4a** proceeds intramolecularly. In addition, the decomposition rate constant of **4a** obtained in this study (k_3 = $4.0\pm0.1\times10^{-5}$ s^{-1} at 120 ℃ in ethylbenzene, see Figure S2d), is in good agreement with the literature data (3×10^{-5} s^{-1} at 120 ℃ in dimethylsulfoxide),[14a,b] which supports the validity of the integrated rate equations 1–3 and the fitting results of the kinetic study.

Finally, the Eyring plots for the dehydrogenation of **1a** under N_2 (k_1 or k_3 vs 1/T in the range of T = 387 to 398 K) are shown in Figures 1c and 1d, from which the activation parameters were determined to be $\Delta H^{\ddagger}$ = 23.8 kcal mol^{-1}, $\Delta S^{\ddagger}$ = −25.2 cal mol^{-1} K^{-1}, and $\Delta G^{\ddagger}_{398\,K}$ = 33.8 kcal mol^{-1} for step 1, and $\Delta H^{\ddagger}$ = 19.8 kcal mol^{-1}, $\Delta S^{\ddagger}$ = −28.2 cal mol^{-1} K^{-1}, and $\Delta G^{\ddagger}_{398\,K}$ = 31.0 kcal mol^{-1} for step 3. Thus, the generation of the benzylic radical is involved in the rate-determining step (Scheme 1, step 1).

The reaction mechanism was further studied by density functional theory (DFT) calculations for the dehydrogenation of **1a** to **2a** (for details, see the Supporting Information).[15] The calculated free-energy profiles are shown in Figure 2.[16] For the generation of the benzylic radical from **1a** by a TEMPO-mediated HAT process, the activation energy was calculated to be 29.2 kcal mol^{-1} (**TS1**), putting this step 17.3 kcal mol^{-1} uphill towards the benzylic radical. The calculated barrier $\Delta G_{(calc)}^{\ddagger}$ = 29.2 kcal mol^{-1} follows reasonably well our experimental value of $\Delta G_{(exp)}^{\ddagger}$ = 33.8 kcal mol^{-1}. After fast trapping of the benzylic radical by TEMPO, two pathways appear to be plausible for the decomposition of the alkoxyamine intermediate **4a**: (i) an intramolecular Cope-type rearrangement (**TS$_{cope}$**; 33.7 kcal mol^{-1}) and (ii) a direct abstraction of a terminal hydrogen atom by TEMPO (**TS$_{intra}$**; 28.2 kcal mol^{-1}), formed by the dissociation of the alkoxyamine C–O bond. From the calculation results, pathway (ii) is more viable because of the following reasons: (a) **TS$_{intra}$** is lower than **TS$_{cope}$**, and (b) the lower value of **TS$_{intra}$** than **TS1** is in good agreement with our kinetic studies from which the benzylic radical generation (Scheme 3, step 1) was suggested to be rate-determining.[17]

CONCLUSION

In summary, we have demonstrated the HAT catalysis of TEMPO which promote the homolytic cleavage of benzylic or allylic C–H bond to give the corresponding alkyl radicals. The dule roles played by TEMPO as a HAT catalyst and a radical scavenger led to the aerobic dehydrogenation of activate alkanes. The key to the selective conversion is attributed to the fast radical trapping by TEMPO, which suppresses the reaction of molecular oxygen with the radical to form oxygenated products. Different from the conventional hydride-transfer catalysis of TEMPO in oxidation reactions, this study will facilitate using TEMPO as a HAT catalyst in organic transformations.

ASSOCIATED CONTENT

Supporting Information. Detailed experimental procedures, Schemes S1 and S2, Figures S1 and S2. This material is available free of charge via the Internet at http://pubs.acs.org."

AUTHOR INFORMATION

Corresponding Authors

Xiongjie Jin – *Department of Chemistry and Biotechnology, Graduate School of Engineering, The University of Tokyo, Bunkyo-ku, Tokyo 113-8656, Japan;* Email: t-jin@g.ecc.u-tokyo.ac.jp

Kyoko Nozaki – *Department of Chemistry and Biotechnology, Graduate School of Engineering, The University of Tokyo, Bunkyo-ku, Bunkyo-ku, Tokyo 113-8656, Japan;* Email: nozaki@chembio.t.u-tokyo.ac.jp

Authors

Tasuku Ito – *Department of Chemistry and Biotechnology, Graduate School of Engineering, The University of Tokyo, Bunkyo-ku, Tokyo 113-8656, Japan*

Falk William Seidel – *Department of Chemistry and Biotechnology, Graduate School of Engineering, The University of Tokyo, Bunkyo-ku, Tokyo 113-8656, Japan*

Notes

The authors declare no competing financial interest.

ACKNOWLEDGMENT

This work was supported by JSPS KAKENHI JP18H05259, JP19K15357, JP20H04803, JP21K18842, JP21H01712 and JST ERATO JPMJER2103.

REFERENCES AND NOTES

[1] de Nooy, A. E. J.; Besemer, A. C.; van Bekkum, H., On the Use of Stable Organic Nitroxyl Radicals for the Oxidation of Primary and Secondary Alcohols. *Synthesis* **1996,** 1153-1176.

[2] Bagryanskaya, E. G.; Marque, S. R. A., Scavenging of Organic C-Centered Radicals by Nitroxides. *Chem. Rev.* **2014,** *114*, 5011-5056.

[3] (a) Sheldon, R. A.; Arends, I. W. C. E., Organocatalytic Oxidations Mediated by Nitroxyl Radicals. *Adv. Synth. Catal.* **2004**, *346*, 1051-1071. (b) Tebben, L.; Studer, A., Nitroxides: Application in Synthesis and in Polymer Chemistry. *Angew. Chem. Int. Ed.* **2011**,*50* 5034-5068. (c) Nutting, J. E.; Rafiee, M.; Stahl, S. S., Tetramethylpiperidine *N*-Oxyl (TEMPO), Phthalimide *N*-Oxyl (PINO), and Related *N*-Oxyl Species: Electrochemical Properties and Their Use in Electrocatalytic Reactions. *Chem. Rev.* **2018**, *118*, 4834-4885. (d) Wang, F.; Stahl, S. S., Electrochemical Oxidation of Organic Molecules at Lower Overpotential: Accessing Broader Functional Group Compatibility with Electron–Proton Transfer Mediators. *Acc. Chem. Res.* **2020,** *53*, 561-574.

[4] There are a few reports on the TEMPO-mediated hydrogen atom transfer, for example: (a) Johnston, L. J.; Tencer, M.; Scaiano, J. C., Evidence for hydrogen transfer in the photochemistry of 2,2,6,6-tetramethylpiperidine *N*-oxyl. *J. Org. Chem.* **1986,** *51*, 2806-2808. (b) Babiarz, J. E.; Cunkle, G. T.; DeBellis, A. D.; Eveland, D.; Pastor, S. D.; Shum, S. P., The Thermal Reaction of Sterically Hindered Nitroxyl Radicals with Allylic and Benzylic Substrates: Experimental and Computational Evidence for Divergent Mechanisms. *J. Org. Chem.* **2002,** *67*, 6831-6834. (c) Coseri, S.; Ingold, K. U., Distinguishing between Abstraction and Addition as the First Step in the Reaction of a Nitroxyl Radical with Cyclohexene. *Org. Lett.* **2004**, *6*, 1641-1643. (d) Zhang, B.; Cui, Y.; Jiao, N., Metal-free TEMPO-catalyzed oxidative C–C bond formation from Csp^3–H bonds using molecular oxygen as the oxidant. *Chem. Commun.* **2012,** *48*, 4498-4500.

[5] Warren, J. J., Tronic, T. A.; Mayer, J. M., Thermochemistry of Proton-Coupled Electron Transfer Reagents and its Implication. *Chem. Rev.* **2010**, *110*, 6961-7001.

[6] (a) Dobereiner, G. E.; Crabtree, R. H., Dehydrogenation as a Substrate-Activating Strategy in Homogeneous Transition-Metal Catalysis. *Chem. Rev.* **2010,** *110*, 681-703. (b) Tang, X.; Jia, X.; Huang, Z., Challenges and opportunities for alkane functionalisation using molecular catalysts. *Chem. Sci.* **2018,** *9*, 288-299.

[7] (a) Lu, H.; Zhang, X. P., Catalytic C–H functionalization by metalloporphyrins: recent developments and future directions. *Chem. Soc. Rev.* **2011**, *40*, 1899-1909. (b) Recupero, F.; Punta, C., Free Radical Functionalization of Organic Compounds Catalyzed by *N*-Hydroxyphthalimide. *Chem. Rev.* **2007**, *107*, 3800-3842.

[8] (a) Iosub, A. V.; Stahl, S. S., Palladium-Catalyzed Aerobic Dehydrogenation of Cyclic Hydrocarbons for the Synthesis of Substituted Aromatics and Other Unsaturated Products. *ACS Catal.* **2016**, *6*, 8201-8213. (b) Khenkin, A. M.; Somekh, M.; Carmieli, R.; Neumann, R., Electrochemical Hydroxylation of Arenes Catalyzed by a Keggin Polyoxometalate with a Cobalt(IV) Heteroatom. *Angew. Chem. Int. Ed.* **2018,** *57*, 5403-5407.

[9] Lv, H.; Laishram, R. D.; Yang, Y.; Li, J.; Xu, D.; Zhan, Y.; Luo, Y.; Su, Z.; More, S.; Fan, B., TEMPO catalyzed oxidative dehydrogenation of hydrazobenzenes to azobenzenes. *Org. Biomol. Chem.* **2020,** *18*, 3471-3474.

[10] Hayashi, M.; Sasano, Y.; Nagasawa, S.; Shibuya, M.; Iwabuchi, Y. 9-Azanoradamantane *N*-Oxyl (Nor-AZADO): A Highly Active Organocatalyst for Alcohol Oxidation. *Chem. Pharm. Bull.* **2011**, *59*, 1570-1573.

[11] (a) Ishii Y.; Nakayama, K.; Takeno, M.; Sakaguchi, S.; Iwahama, T.; Nishiyama, Y. A Novel Catalysis of *N*-Hydroxyphthalimide in the Oxidation of Organic Substrates by Molecular Oxygen. *J. Org. Chem.* **1995**, *60*, 3394-3395. (b) Ishii, Y.; Sakaguchi, S.; Iwahama, T. Innovation of Hydrocarbon Oxidation with Molecular Oxygen and Related Reactions. *Adv. Synth. Catal.* **2001**, *343*, 393-427.

[12] (a) Amorati, R.; Lucarini, M.; Mugnaini, V.; Pedulli, G. F.; Minisci, F.; Recupero, F.; Fontana, F.; Astolfi, P.; Greci, L.,

Hydroxylamines as Oxidation Catalysts: Thermochemical and Kinetic Studies. *J. Org. Chem.* **2003,** *68*, 1747-1754. (b) Minisci, F.; Recupero, F.; Cecchetto, A.; Gambarotti, C.; Punta, C.; Paganelli, R.; Pedulli, G. F.;Fontana, F., Solvent and Temperature Effects in the Free Radical Aerobic Oxidation of Alkyl and Acyl Aromatics Catalysed by Transition Metal Salts and *N*-Hydroxyphthalimide: New Processes for the Synthesis of p-Hydroxybenzoic Acid, Diphenols, and Dienes for Liquid Crystals and Cross-Linked Polymers. *Org. Proc. Res. Dev.* **2004,** *8*, 163-168. (c) Cai, Y.; Koshino, N.; Saha, B.; Espenson, J. H., Kinetics of Self-Decomposition and Hydrogen Atom Transfer Reactions of Substituted Phthalimide *N*-Oxyl Radicals in Acetic Acid. *J. Org. Chem.* **2005,** *70*, 238-243.

[13] Nagasawa, S.; Sasano, Y.; Iwabuchi, Y., Synthesis of 1,3-Cycloalkadienes from Cycloalkenes: Unprecedented Reactivity of Oxoammonium Salts. *Angew. Chem. Int. Ed.* **2016**, *55*, 13189-13194.

[14] (a) Li, I.; Howell, B. A.; Matyjaszewski, K.; Shigemoto, T.; Smith, P. B.; Priddy, D. B. Kinetics of Decomposition of 2,2,6,6-Tetramethyl-1-(1-phenylethoxy)piperidine and Its Implications on Nitroxyl-Mediated Styrene Polymerization. *Macromolecules*, **1995**, *28*, 6692–6693. (b) Greszta, D.; Matyjaszewski, K. *Macromolecules*, **1996**, *29*, 7661–7670. (c) Shang, Y.; Jie, X.; Jonnada, K.; Zafar, S. N.; Su, W., Dehydrogenative desaturation-relay via formation of multicenter-stabilized radical intermediates. *Nat. Commun.* **2017,** *8*, 2273.

[15] Neese, F., Software update: the ORCA program system, version 4.0. *WIREs Comput. Mol. Sci.* **2018,** *8*, e1327.

[16] Due to the strong static electron correlation (SEC) in several structures (as denoted by the fractional occupation number weighted electron density (FOD); as a guideline, FOD values of >0.2 are expected to be problematic for single reference techniques), Grimme *et al.*'s finite temperature method was applied, which has been previously shown to adequately follow energy curves at the fully multireference treated CASSCF/NEVPT2 level of theory for reactions affected by strong SEC effects. (a) Grimme, S.; Hansen, A., A Practicable Real-Space Measure and Visualization of Static Electron-Correlation Effects. *Angew. Chem. Int. Ed.* **2015,** *54*, 12308-12313. (b) Bauer, C. A.; Hansen, A.; Grimme, S., The Fractional Occupation Number Weighted Density as a Versatile Analysis Tool for Molecules with a Complicated Electronic Structure. *Chem. Eur. J.* **2017,** *23*, 6150-6164.

[17] The barrier for $\mathbf{TS}_{\mathbf{intra}}$ appears underestimated by the static DFT approach due to the expected error of the calculations as indicated by the low calculated $\Delta G_{(calc;\ intra)}^{\ddagger}$ = 21.2 kcal mol^{-1}, which is likely due to the required pre-equilibrium reaction of the TEMPO dissociation from **4a** and following diffusion processes, and competitive radical trapping of the benzylic radical by the excess TEMPO. (a) Goerigk, L.; Hansen, A.; Bauer, C.; Ehrlich, S.; Najibi, A.; Grimme, S., A look at the density functional theory zoo with the advanced GMTKN55 database for general main group thermochemistry, kinetics and noncovalent interactions. *Phys. Chem. Chem. Phys.,* **2017,** *19*, 32184-32215. (b) Caldeweyher, E.; Ehlert, S.; Hansen, A.; Neugebauer, H.; Spicher, S.; Bannwarth, C.; Grimme, S., A generally applicable atomic-charge dependent London dispersion correction. *J. Chem. Phys.,* **2019,** *150*, 154122.

- **TEMPO as the HAT catalyst**
- **Transition-metal free dehydrogenation**